Introduction

The understanding of warped galaxies has been enriched those last years by ideas such as galactic infall (Ostriker & Binney 1989; Jiang & Binney 1999) or dynamical friction between the halo and the disk (Debattista & Sellwood 1999). In spite of the fact that the evidences for non-self-gravitating HI disks are actually weak (Arnaboldi et al. 1997; Becquaert & Combes 1997), most of works on the subject are built on the assumption of a disk embedded in a fat spheroidal or triaxial halo.

Through N-body simulations, this work presents two methods of getting warped self-gravitating galactic disks. The first one imports inclined angular momentum through material accretion and the second one uses an outer warped potential. A ring decomposition allows to study the evolution of the disks, in particular the shape of the line of nodes (LON).

N-Body disk model

The N-body disk is based on a superposition of three Miyamoto-Nagai potentials :

$$\Phi(R,\phi,z) = -\sum_{i=1}^{3} \frac{GM_i}{\sqrt{R^2 + \left(a_i + \sqrt{z^2 + b_i^2}\right)^2}}$$

component	a_i	b_i	GM_i
bulge	0	0.5	0.066
visible disk	2.16	0.5	0.0171
gas disk	8.33	0.5	0.763

The three components can be viewed as representing a bulge, a visible disk and a gas disk. Note that GM_i represents the fraction of the total mass. In simulation 1, the disk contents 10^6 particles of equal mass when simulations 2 contents 10^5. Both are run with the Barnes-Hut treecode parallelized to run on the Geneva Observatory 132 processors Beowulf cluser. The time unit is in Myr.

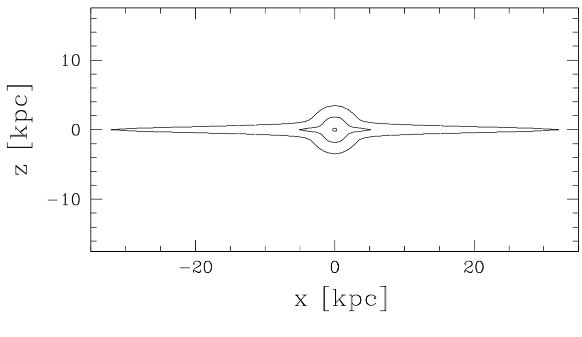

Isodensity curves of the disk model.

Ring decomposition

In order to represent the warped galactic disk, we have decomposed it in a family of concentric rings. The position of one ring is determined by two angle ϕ and θ, respectively the precession and the nutation angle of the normal of the ring $\vec{n}$ (see figure).

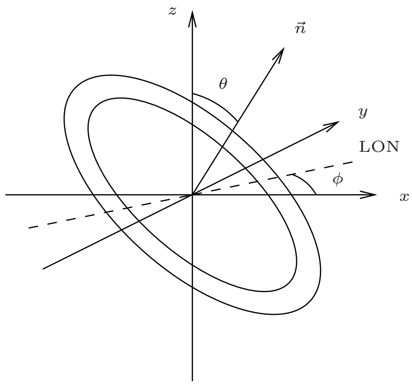

The evolution of the warped disk is represented with two plots.

- The **Tip-LON** plot (Briggs 1990), where each point represents the projection of the normal of one ring (see figure). ϕ is read along the circles from 0 to 360°, while θ is read perpendicularly to those circles which correspond to $\theta = 10°$ and $\theta = 20°$.
- The $\boldsymbol{\theta}$ **vs** $\boldsymbol{R}$ plot.

The plane of projection is defined to be the best fit plane of the inner parts of the galaxy. The direction of one ring is determined either by the positions of particles (black on the plots) or by their velocities (red on the plots).

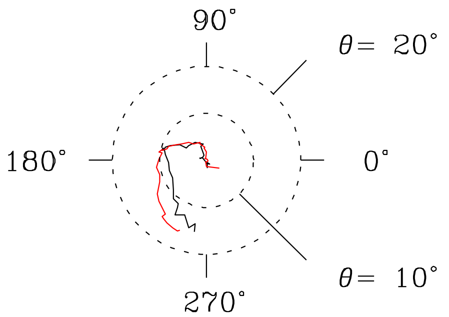

Tip-LON plot

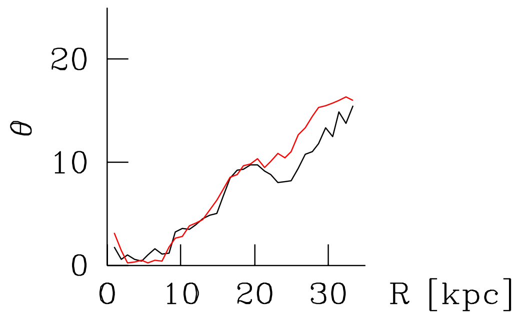

θ vs R plot

Simulation 1 : external potential

In this simulation, the galactic disk is embedded in a non-rotating warped potential during a perturbation time (0 to 577 Myr). The initially flat disk is also driven and develops a warp.

The outer potential is obtained by replacing z by $z - wR^2 \cos\phi$ in the galactic disk potential. w is a parameter determining the amplitude of the warp. To drive adiabatically the disk, the outer potential is flat at the beginning of the simulation ($w = 0\,\mathrm{kpc}^{-1}$) and warps slowly during the perturbation time, rising the maximum deformation with $w = 0.015\,\mathrm{kpc}^{-1}$. During the perturbation, the mass contribution of the disk and the outer potential are equal. The total length of the simulation is 1616 Myr.

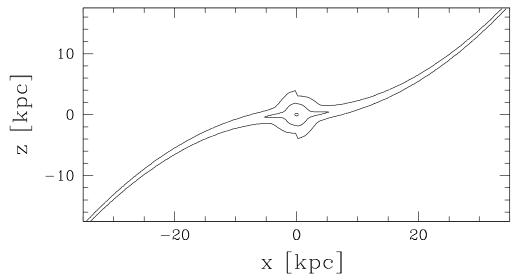

Isodensity curves of the outer warped potential at its maximum deformation ($w = 0.015\,\mathrm{kpc}^{-1}$).

Evolution of the disk

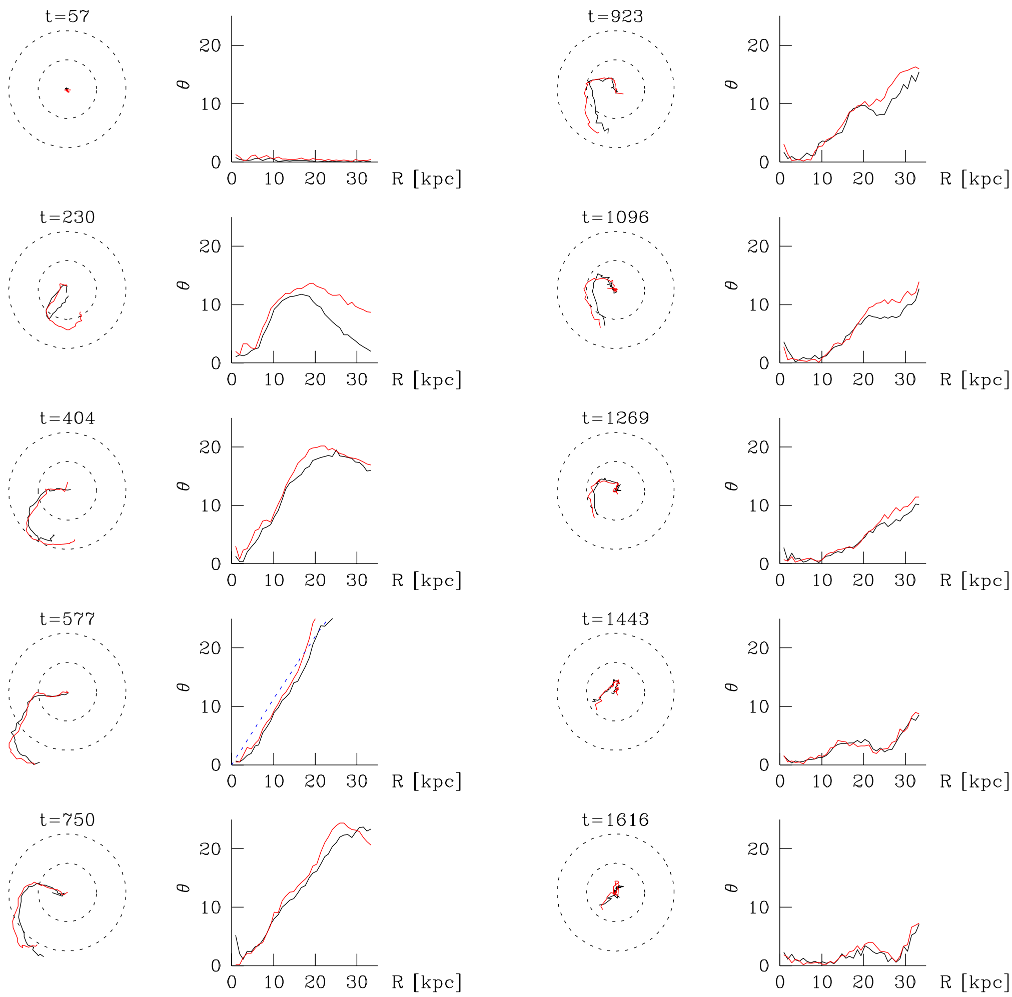

- The outer potential has rapidly an influence over the inner regions ($t = 230\,\mathrm{Myr}$ while the outer regions remain nearly flat. Note the difference between red (velocities) and black (positions) data.
- At ($t = 404\,\mathrm{Myr}$ a leading LON is clearly visible and will persist till ($t = 1269\,\mathrm{Myr}$).
- At ($t = 577\,\mathrm{Myr}$, the deformation reaches his maximum and is equivalent to the warp of the outer potential (blue dashed line).
- After the end of the perturbation the amplitude of the warp declines and a disk forms at the center ($t = 923\,\mathrm{Myr}$) the one will extends during the next Myr.
- At the end of the simulation ($t = 1443$ to $1616\,\mathrm{Myr}$) the outer parts which are always slightly tipped, form a straight LON.

The cylindrical slices presented on the following diagram show the increasing and decreasing of the warp. The amplitude of the warp in respect of the azimuth is well described with a cosine function. The heating of the disk (z dispersion) due to the accretion is clearly visible. The width of one slice is about $0.9\,\mathrm{kpc}$.

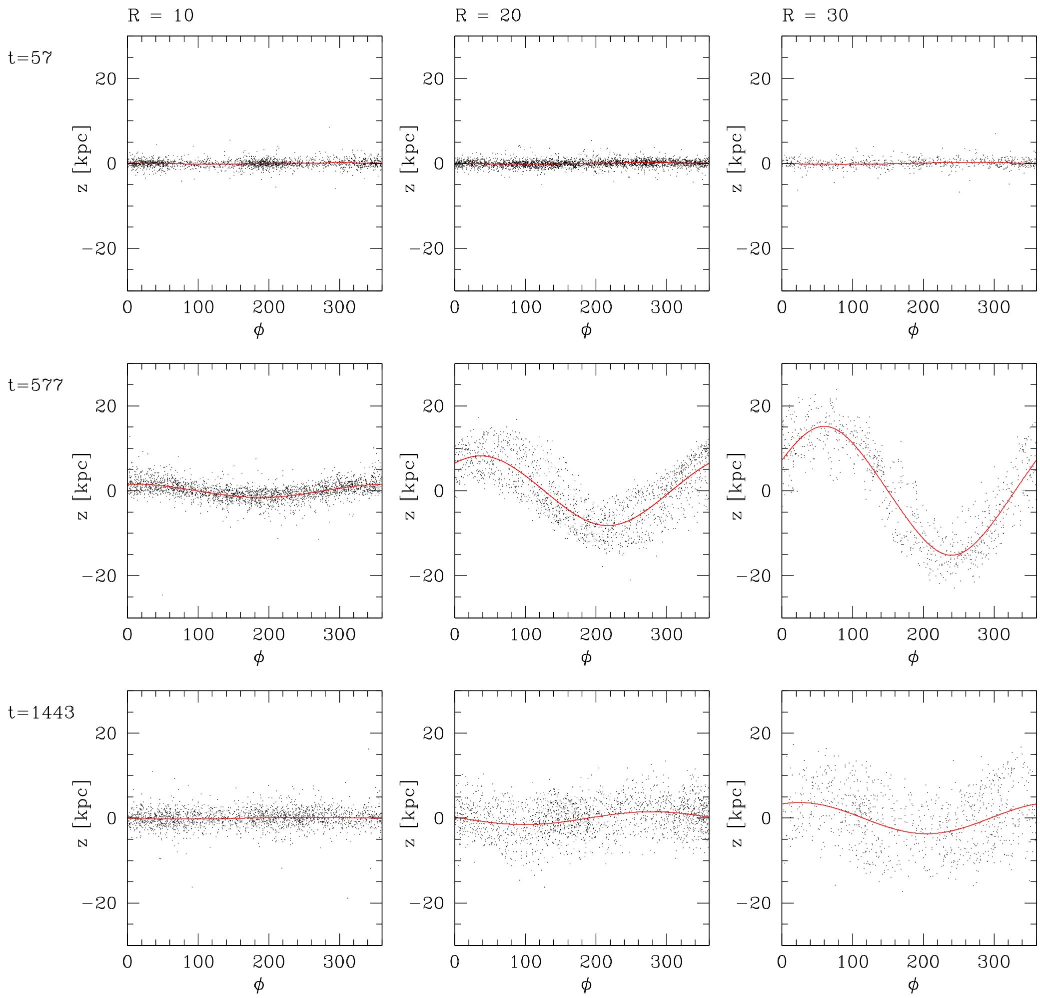

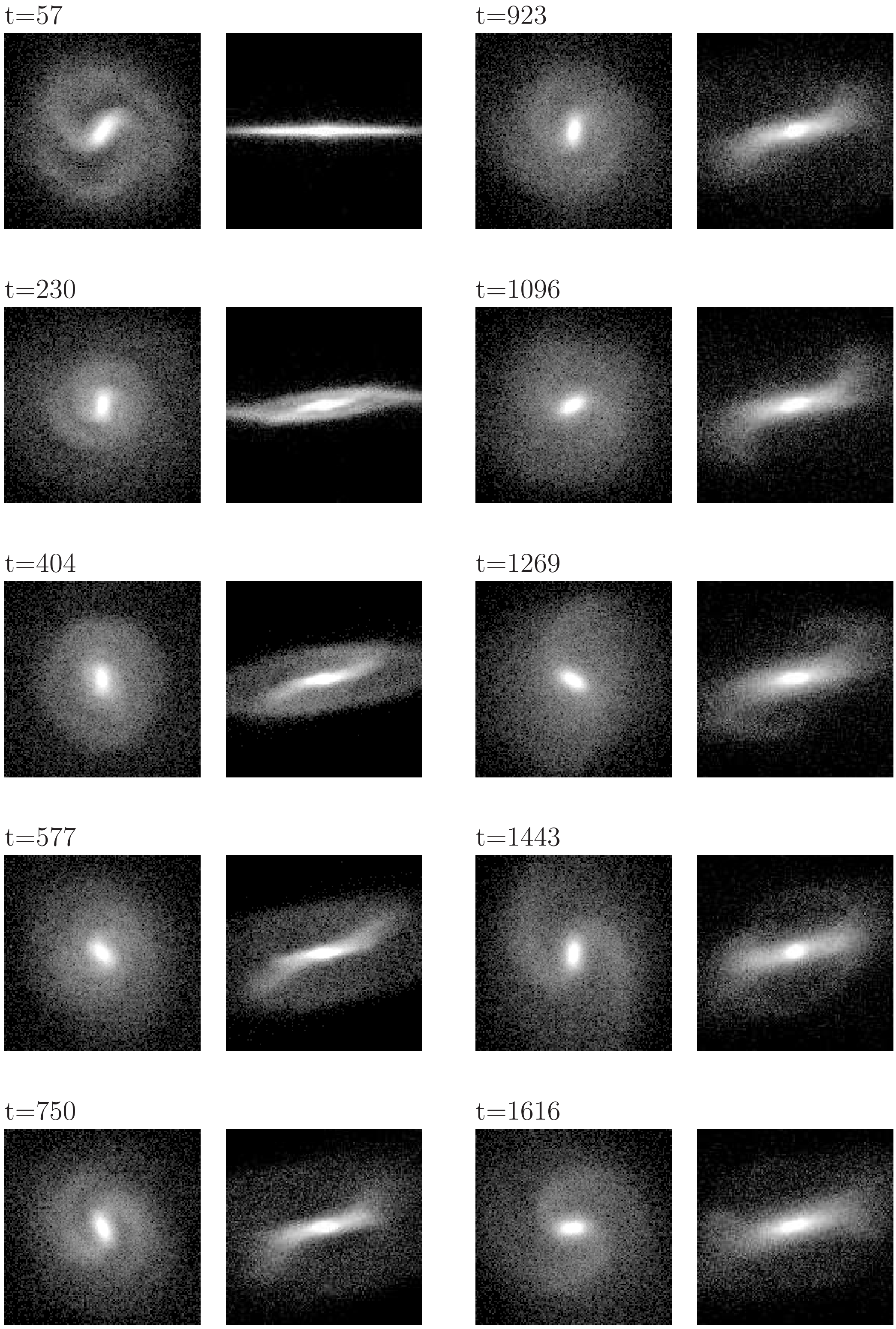

Face-on and edge-on film of the simulation. Each square represents 60 kpc.

Simulation 2 : accretion

In this simulation, the warp is generated by material accretion. This idea has been suggested by Ostriker & Binney (1989) and tested by Jiang & Binney (1999) in a simulation where a ring disk is embedded in an oblate N-body halo. The originality of the present simulation is the absence of the halo. The infall of material is obtained following the method of Jiang & Binney (1999), which consists of injecting particles in an inclined tork.

The tork is slowly rotating from 10 to 60 degrees round the y axis (see figure on the right). Particles are injected only during the first 1924 Myr with a constant rate. There velocity is slightly lower than the velocity given by the rotation curve at an equivalent radius, and the total injected mass represent 100 % of the mass of the initial galactic disk. The total length of the simulation is 2539 Myr

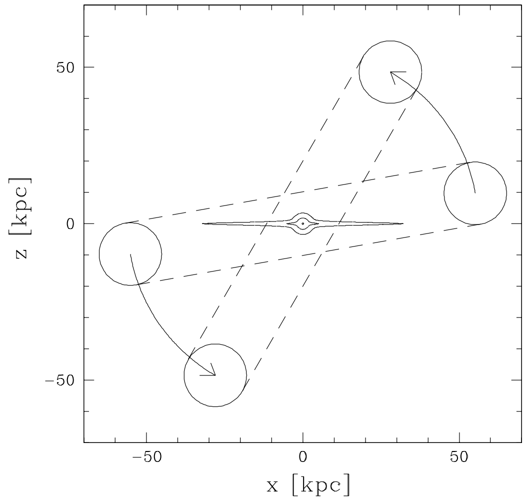

Evolution of the disk

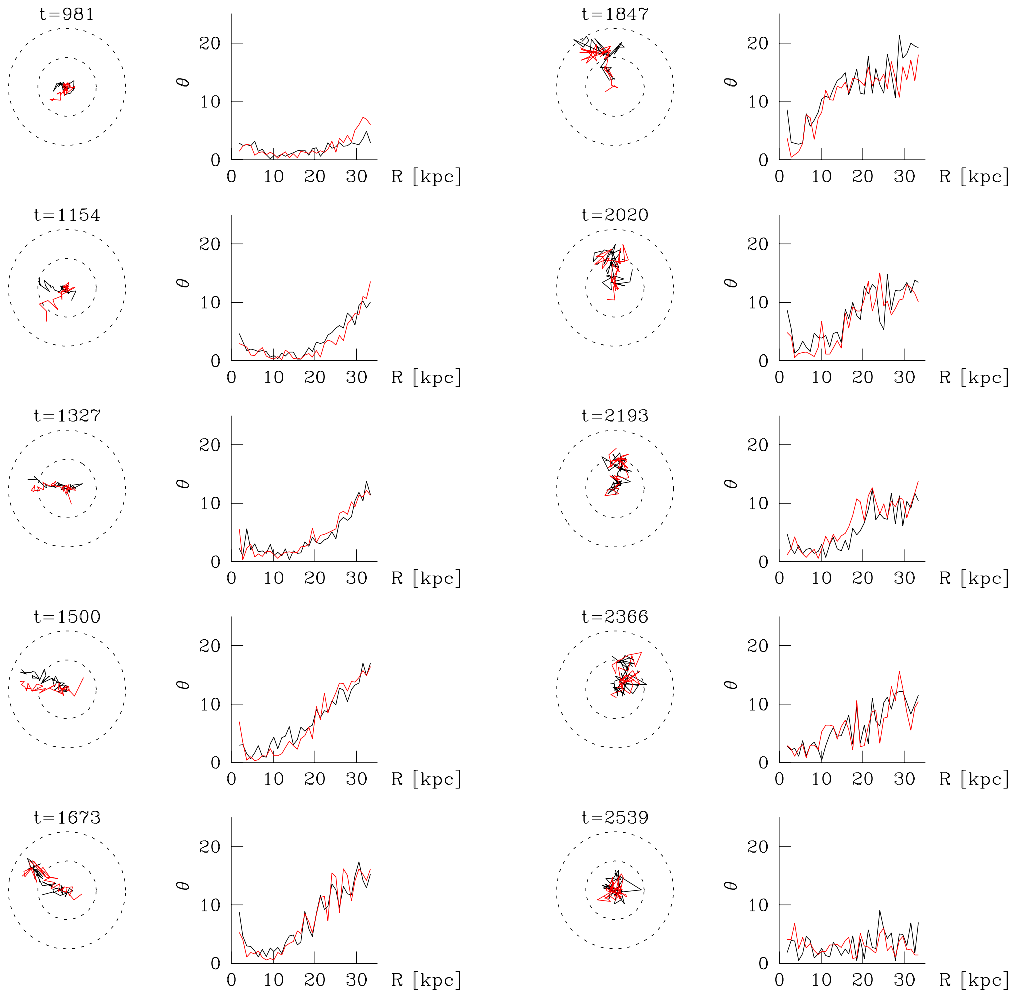

- The effect of accretion is perceptible only after about 1 Gyr. The disk remains flat before.
- At $t = 1154$ Myr the Tip-LON plot shows two LON, one is given by the velocities (red) and the other by the positions (black).
- During the following steps, the amplitude of the warp increases and a straight LON is clearly visible.
- Between $t = 1154$ Myr and $t = 2020$ Myr we observe a retrograde rotation of the LON, which is coherent with the flat geometry of the galaxy.
- After the end of accretion ($t = 1924$ Myr) the warp decrease slowly and became flat again at $t = 2539$ Myr.

The cylindrical slices presented on the bottom diagram show the increasing and decreasing of the warp. The amplitude of the warp in respect of the azimuth is quite well described with a cosine function. The heating of the disk (z dispersion) due to the accretion is clearly visible. The width of one slice is about 1.8 kpc.

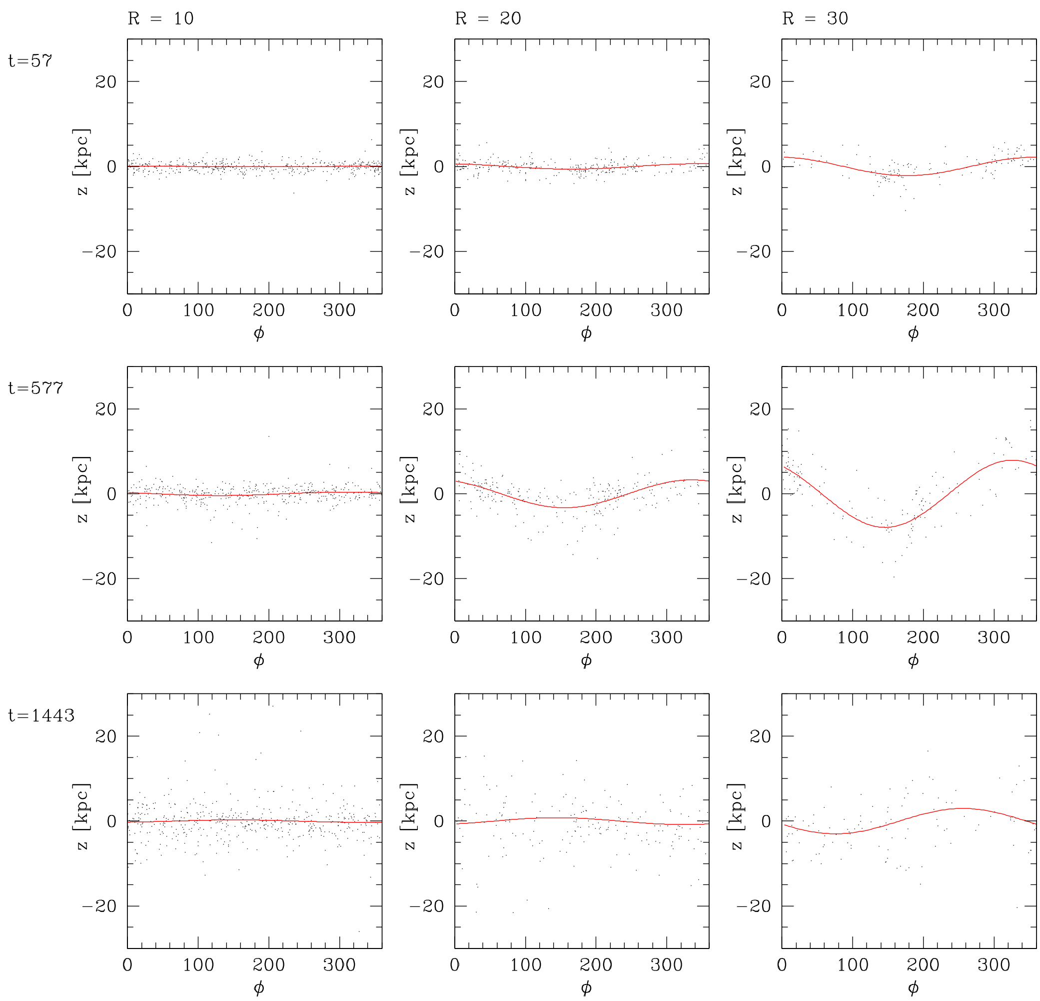

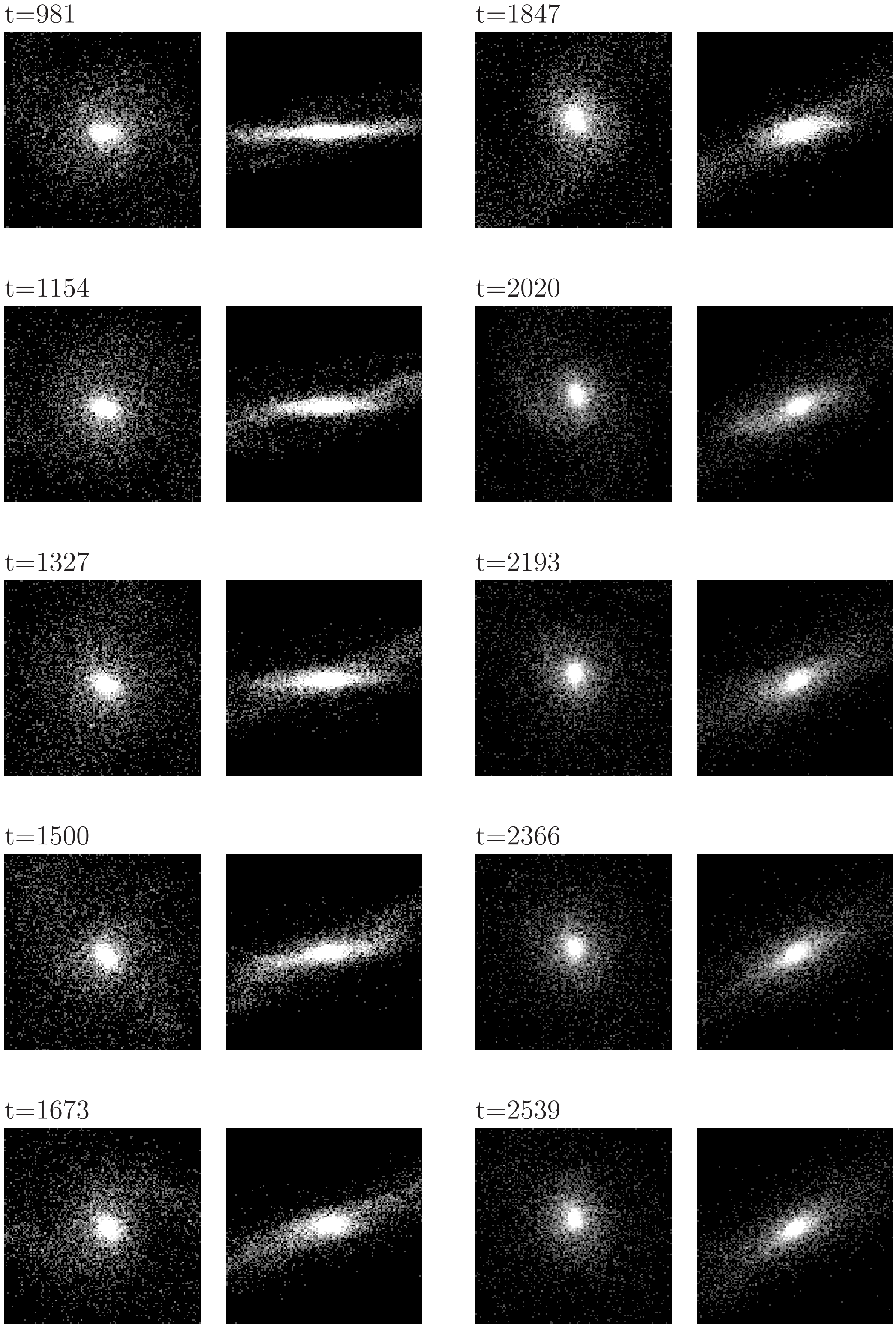

Face-on and edge-on film of the simulation. Each square represents 60 kpc.

Discussion

The perturbation type determines strongly the shape of the disk. In the first simulation, the deformation occurs from the inner regions to the outer whereas it occurs from the outer to the inner in the second one. This has two observed effects :

- The shape of the LON is significantly different. A **leading LON** is generated in presence of an outer potential, which can be assimilated to a warped heavy DM disk. A similar result has been found by Debattista & Sellwood (1999) in the case of dynamical friction between a spherical misaligned rotating halo and a disk. This leading LON persists during about 1 Gyr and becomes straight when the warp decreases. In contrary, a **straight rotating LON** is generated with accretion.

- The birth of the warp is also quite different. In case of our outer potential, the inner regions felt its gravity faster and tip before the outer ones. A large abrupt warp can be quickly observed, even if the outer regions lie always on the initial plane (see next figure). This effect is not present in case of accretion, where the inner regions remain flat while the outer ones tip. Studies of HI in warped edge-on galaxies could also give valuable information on the way the disk becomes warped.

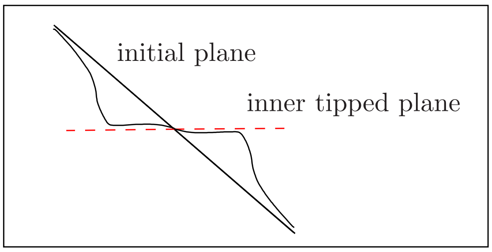

Finally, this work shows that appreciable warps can be observed during more than 1 Gyr, even in the absence of a halo.

References

[1] Arnaboldi M., Oosterloo T., Combes F. et al., 1997, AJ, 113, 585

[2] Becquaert J.-F., Combes F., 1997, A&A, 325, 41

[3] Briggs F.H., 1990, ApJ, 352, 15

[4] Debattista V., Sellwood J., 1999, ApJ, 513,L107

[5] Jiang I-G., Binney J., 1999, MNRAS, 303, L7-L10

[6] Ostricker E.C., Binney J., 1989, MNRAS, 237,785